Non-homentropic flow generated by trains in tunnels with side branches

M.J.P. William-Louis and C. Tournier

LAMIH, Université de Valenciennes, Valenciennes Cedex, France

Received November 1995
Revised September 1997

Nomenclature

c	=	speed of sound
cf	=	friction factor
c_v	=	specific heat at constant pressure
h	=	specific enthalpy
p	=	pressure
r	=	perfect gas constant
s	=	entropy
t	=	time
u	=	mean flow velocity
x	=	spatial coordinate
A	=	cross section
D_h	=	hydraulic diameter
Q	=	mass flow rate
T	=	temperature
V_{tr}	=	train speed
γ	=	specific heat ratio
λ	=	Riemann variable
ρ	=	density
ξ	=	stagnation pressure loss coefficient

Subscripts

a	=	adiabatic
tr, tun	=	train, tunnel
o, oi	=	initial state, stagnation state

Introduction

With the development of high speed trains, aerodynamic problems related to the circulation of trains in tunnels is currently a subject of great importance. When a train enters a tunnel, large pressure fluctuations are produced and propagated through the tunnel as waves. These waves affect the comfort of passengers (unless the train is sealed) as well as the structural integrity of equipment in the tunnel. The flow generated is unsteady and largely one dimensional with local regions of three dimensional flow at the ends of the train, tunnel portals and the air shaft junctions. A three dimensional simulation would be very demanding in regard to the combined effects of unsteadiness, compressibility and the turbulent behaviour of the flow and would involve a high level of numerical resolution. The problem has been investigated by many authors. The studies undertaken are essentially based on one-dimensional models, which can be fairly sophisticated, and take account of a large number of effects (compressibility, wall friction, heat exchange, wall porosity, etc.). These theoretical models can be classified into six categories: the non-homentropic flow model, the homentropic flow model, the isentropic flow model, the constant density and finite speed of sound model, the unsteady incompressible flow model and finally the quasi-steady incompressible flow model. The models are described in Woods and Pope (1979) and details given of their range of validity. The most sophisticated are the homentropic and the non-homentropic approaches.

International Journal of Numerical Methods for Heat & Fluid Flow
Vol. 8 No. 2, 1998, pp. 183–198.

In the homentropic model, the continuity and motion equations are used in conjunction with the law of Laplace, $\frac{p}{\rho^{\gamma}} = cste$. Such an approach has been used to predict the flow generated by the circulation of one or two trains in single or double-track tunnels. The relative simplicity of the model means that it led itself to extension to provide predictions for multiple train movements in complex tunnel networks (Fox and Henson, 1971; Fox and Vardy, 1973; Henson *et al.*, 1982; Vardy, 1976). The results give good predictions of the behaviour of pressure and the mean velocity of the air with time. However, in this model, one cannot take into account the heat exchange and consequently, the predicted temperature field is unrealistic, particularly for high speed trains and long tunnels.

In the non-homentropic flow model, the conservation of mass, momentum and energy are used with the full thermodynamic relationship of state ($\frac{p}{\rho} = rT$). The model is academically rigorous and has been used to simulate the circulation of one train in a single-track tunnel (Pope, 1986; Woods and Pope, 1981). The approach, however, suffers from the disadvantage of being difficult to extend to complex tunnel configurations and passing trains. This extension was attempted by Waclawicek and Sockel (1982) but they assumed isentropic flow for the ends of the train while passing the shaft. Their method was applied to predict the effects of airshafts in alleviating pressure transients and the results confirmed the earlier studies due to Vardy (1976).

The purpose of this paper is to present an extension of the fully non-homentropic approach to the case of tunnels with side branches and an application on the prediction of the influence of airshafts on the pressure waves.

General considerations

Away from the locations where three dimensional effects are dominant (tunnel and train ends, junctions, abrupt changes in cross section, etc.), the flow can be assumed to be one-dimensional. In these zones, the equations of one dimensional gas dynamics (continuity, momentum and energy), expressed with u, c and a as the variables can be used. The introduced variable, a, is equivalent to a celerity and characterises the entropy changes (Pichard, 1989):

$$a = c_0 \exp\left(\frac{\Delta s}{2c_p}\right) \tag{1}$$

This, combined with the full thermodynamic relationship, gives the state relations:

$$\frac{p}{p_0} = \left(\frac{c}{a}\right)^{\frac{2\gamma}{\gamma-1}} \quad \frac{\rho}{p_0} = \frac{\gamma}{a^2}\left(\frac{c}{a}\right)^{\frac{2}{\gamma-1}} \quad and \quad T = \frac{c^2}{\gamma r} \tag{2}$$

With these relations, the governing equations (continuity, momentum, and energy) for the flow become:

$$\begin{cases} \dfrac{1}{c}\dfrac{dc}{dt} - \dfrac{\gamma}{a}\dfrac{da}{dt} + \dfrac{\gamma-1}{2}\dfrac{\partial u}{\partial x} + \dfrac{\gamma-1}{2}\dfrac{u}{A}\dfrac{dA}{dx} & = 0 \\ \dfrac{du}{dt} + \dfrac{2}{\gamma-1}c^2\left(\dfrac{1}{c}\dfrac{\partial c}{\partial x} - \dfrac{1}{a}\dfrac{\partial a}{\partial x}\right) + F & = 0 \\ \dfrac{1}{a}\dfrac{da}{dt} - \dfrac{\gamma-1}{2c^2}\left(P + \dot{Q}\right) & = 0 \end{cases} \tag{3}$$

Where F is, as the case may be, the wall friction force per mass unit in the empty parts of the tunnel, and in the annulus between train and tunnel walls:

$$F = \begin{cases} \dfrac{1}{2} cf_{tun} u|u| \pi \dfrac{D_{htun}}{A_{tun}} & \textit{(empty tunnel)} \\ \dfrac{1}{2} \dfrac{cf_{tun} u|u| \pi D_{htun} + cf_{tr}(u - V_{tr})|u - V_{tr}| \pi D_{htr}}{(A_{tun} - A_{tr})} & \textit{(annulus)} \end{cases}$$

It has to be noted that in this expression, the friction coefficients on the tunnel and train walls have to be given. Generally, they are taken as constants from experimental results. In this way, the numerical calculation gives realistic results when compared with measurement. The flow, however, is unsteady and the air compressible. The pressure waves can modify the boundary layer locally causing the friction factor to vary with time. This has been investigated and unsteady models developed. The models, however, have failed to give much improvement in the predictions of the pressure fluctuations (Schultz and Sockel, 1988; William-Louis *et al.*, 1993). In the present paper, these coefficients are, therefore, taken to be constant.

In the system of equations (3), the work done by the friction force per unit time, F, for the empty tunnel and in the annulus is given by:

$$P = uF - \begin{cases} 0 & \textit{(empty tunnel)} \\ \dfrac{cf_{tr} V_{tr}(u - V_{tr})|u - V_{tr}| \pi D_{htr}}{2(A_{tun} - A_{tr})} & \textit{(annulus)} \end{cases}$$

and the heat exchanges at the walls by:

$$\dot{Q} = \frac{\gamma r |u| \pi}{2(\gamma - 1)} \begin{cases} \dfrac{cf_{tun} D_{htun}(T_{tun} - T_{atun})}{A_{tun}} & \textit{(empty tunnel)} \\ \dfrac{cf_{tun} D_{htun}(T_{tun} - T_{atun}) + cf_{tr} D_{htr}(T_{tr} - T_{atr})}{(A_{tun} - A_{tr})} & \textit{(annulus)} \end{cases}$$

The heat transfer coefficients are given as function of the friction factor by using the Reynolds analogy (Hammitt, 1975).

System (3) is solved by the classical characteristics method which gives the compatibility relations along physical characteristics $C^{\pm}$ and the particle pathline C^0:

$$\begin{cases} d\left(\frac{c}{a}\right) \pm \frac{\gamma-1}{2} d\left(\frac{u}{a}\right) = d\lambda^{\pm} \\ \frac{1}{a}\frac{da}{dt} = \frac{\gamma-1}{2c^2}\left(P+\dot{Q}\right) \end{cases} \quad (4)$$

where the variation of the Riemann variable is given by:

$$d\lambda^{\pm} = \left[-\frac{\gamma-1}{2A}\frac{cu}{a}\frac{dA}{dx} + \frac{1}{a}\frac{da}{dt}(\gamma-1)\left(\frac{c}{a} \mp \frac{u}{2a}\right) \mp \frac{\gamma-1}{2}\frac{F}{a}\right] dt$$

The second term in the variation of the Riemann variable represents the influence of the entropy changes on the disturbance characteristics $C^{\pm}$ and $\frac{1}{a}\frac{da}{dt}$ is calculated by using the third relation in the system (4).

Boundary conditions

The one-dimensional approach for predicting the flow generated by a train in a tunnel involves the use of many boundary conditions. The zones, where the flow is highly three dimensional, and the contact surfaces, which are formed at the interfaces between air drawn in from outside and originating from within the tunnel, are treated as boundaries. The conditions across the boundaries are linked to the characteristics relations using the equations of one dimensional gas dynamics. In view of the large number of these boundaries, it is not practicable to present the treatment of all of them in this paper, particularly since the boundary conditions for the circulation of trains in simple tunnels are stated in Pope (1986). The main feature of this paper is the extension of the non-homentropic model to the case of tunnels with side branches. Emphasis will, therefore, be given to the boundary conditions for a junction. The boundary conditions take into consideration the wave propagation behaviour at the junction, the interaction of the train ends with the junction as they pass, the contact surface and the contact surface-junction interaction. These features are discussed in the following sections.

Wave-junction interaction

During the propagation of pressure waves in tunnels with airshafts, the waves can disturb the flow at the junction where a joining, dividing or no flow condition can prevail. In the propagation process, it is necessary to consider all these cases when predicting the flow upstream and downstream of the junction at time $t+\Delta t$ from a knowledge of u, c and a at t.

In order to present the principle which is used, consideration will be given to a joining flow in a junction (Figure 1). In the one-dimensional approach, the behaviour of the flow within the control volume cannot be modelled explicitly. However, it is possible to use a one-dimensional model, if the average flow upstream and downstream of the junction only is of interest. In this case, the control volume is assumed to be infinitesimal and the wave travel time across it

instantaneous. The three dimensional effects within this control volume are modelled implicitly using empirical stagnation pressure loss coefficients for the branches of the junction as is common practice in the solution of steady pipe flow problems. The flow within the control volume is treated as adiabatic. The construction of the physical characteristics at the boundaries of the control volume is as follows.

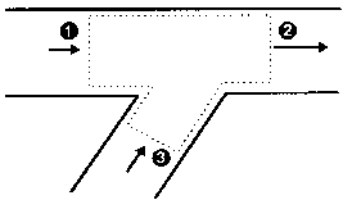

Figure 1.
Joining flow

At section 1 (inlet), the physical characteristics and the pathline are defined with the compatibility relations along these curves giving:

$$d\left(\frac{c}{a}\right)_1 + \frac{\gamma-1}{2} d\left(\frac{u}{a}\right)_1 = d\lambda_1^+ \quad \text{and} \quad \frac{1}{a_1}\left(\frac{da}{dt}\right)_1 = \frac{\gamma-1}{2c_1^2}\left(P+\dot{Q}\right)_1 \tag{5,6}$$

At section 3 (inlet), the two compatibility relations are given by:

$$d\left(\frac{c}{a}\right)_3 - \frac{\gamma-1}{2} d\left(\frac{u}{a}\right)_3 = d\lambda_3^- \quad \text{and} \quad \frac{1}{a_3}\left(\frac{da}{dt}\right)_3 = \frac{\gamma-1}{2c_3^2}\left(P+\dot{Q}\right)_3 \tag{7,8}$$

At section 2, out flow exists which makes the pathline undefined. The physical characteristics C_2^-, however, is given by:

$$d\left(\frac{c}{a}\right)_2 - \frac{\gamma-1}{2} d\left(\frac{u}{a}\right)_2 = d\lambda_2^- \tag{9}$$

By assuming that the flow in the control volume is quasi-steady, we also have the following relations:

- the mass conservation

$$Q_1 + Q_3 = Q_2 \tag{10}$$

- the stagnation enthalpy balance

$$Q_1 h_{01} + Q_3 h_{03} = Q_2 h_{02} \tag{11}$$

- the stagnation pressure loss respectively between sections 1-2 and 3-2:

$$p_{01} - p_{02} = \frac{1}{2}\rho_2 u_2^2 \xi_{12} \quad \text{and} \quad p_{03} - p_{02} = \frac{1}{2}\rho_2 u_2^2 \xi_{32} \tag{12,13}$$

Finally, the equations (5-13) give a non-linear system and the solution is formed by the variables u, c and a at sections 1, 2, and 3 at time $t+\Delta t$.

Train-junction interaction

When the train reaches the junction, different configurations, which must be regarded as specific boundary conditions, are involved. These comprise the train nose-junction, train rear-junction and train body-junction interactions. In all these cases, the generated flow is very complex and here, too, assumptions are needed when using the one-dimensional approach. As the length occupied by the junction and the length of the train ends are negligible in regard of the distance covered by the waves during the time step Δt, these zones can be assumed to be infinitesimal. The temporal shift introduced by this assumption is negligible.

Considering the train nose, for example, the sections involved for the calculations are:

- L and R, sections at the beginning of the annulus and at the nose front;
- 1, 2 and 3, sections defined in Figure 1.

Noting that the flow displacement effect of the nose generates a dividing flow in the junction, the construction of the characteristics curves shows two cases (see Figure 2), and for each case, only four sections are involved in the calculation: L, R, 2 and 3 for case (a), and 1, L, R and 3 for case (b). In the zones L-R and 1-2-3, the three dimensional effects are important but only the variables upstream and downstream of each zone are of interest. As a result, the flow in these zones is assumed to be quasi-steady. Details of the solution of the boundary conditions are given as follows.

In the zone L-R, the equations governing the conservation of mass, the enthalpy balance and the pressure loss are expressed in a frame of reference relative to train. If the case of a train-nose interaction is considered with heat release, L-R must be divided into two domains, L-L' and L'-R. In the part L-L', a Rayleigh flow treatment is applied and within L'-R the flow is assumed to be adiabatic. Details for a train-nose with heat release are stated in Woods and Pope (1981) and Pope (1986). In this paper, only adiabatic flow over the nose is considered.

In the zone 1-2-3, the relationships governing the conservation of mass and the pressure losses are used. Noting that there is an adiabatic dividing flow in

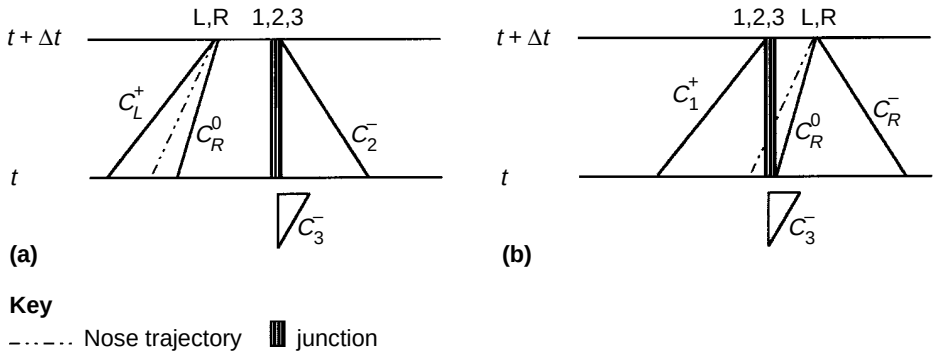

Figure 2.
Characteristics construction

the junction, the specific stagnation enthalpy at section 1, 2 and 3 can be considered equal.

These relationships are solved in conjunction with the compatibility conditions on each side of the boundary except the relations along the characteristics between the train boundary and the junction (C_R^- for case (a) and C_L^+ for case (b)). Finally, this boundary is modelled respectively for case (a) and (b) by the systems:

$$\begin{cases} d\left(\frac{c}{a}\right)_L + \frac{\gamma-1}{2} d\left(\frac{u}{a}\right)_L = d\lambda_L^+ \\ \frac{1}{a_R}\left(\frac{da}{dt}\right)_R = \frac{\gamma-1}{2c_R^2}\left(P+\dot{Q}\right)_R \\ d\left(\frac{c}{a}\right)_2 - \frac{\gamma-1}{2} d\left(\frac{u}{a}\right)_2 = d\lambda_2^- \\ d\left(\frac{c}{a}\right)_3 - \frac{\gamma-1}{2} d\left(\frac{u}{a}\right)_3 = d\lambda_3^- \\ Q'_L = Q'_R \\ h'_{0L} = h'_{0R} \\ p_{0R} - p_{0L} = \rho_L (u_L - V_{tr})^2 \xi_{nt}/2 \\ Q_R = Q_2 - Q_3 \\ p_{0R} - p_{02} = \rho_2 u_2^2 \xi_{12}/2 \\ p_{0R} - p_{03} = \rho_3 u_3^2 \xi_{13}/2 \\ h_{0R} = h_{02} = h_{03} \end{cases} \quad \text{and} \quad \begin{cases} d\left(\frac{c}{a}\right)_1 + \frac{\gamma-1}{2} d\left(\frac{u}{a}\right)_1 = d\lambda_1^+ \\ \frac{1}{a_R}\left(\frac{da}{dt}\right)_R = \frac{\gamma-1}{2c_R^2}\left(P+\dot{Q}\right)_R \\ d\left(\frac{c}{a}\right)_R - \frac{\gamma-1}{2} d\left(\frac{u}{a}\right)_R = d\lambda_R^- \\ d\left(\frac{c}{a}\right)_3 - \frac{\gamma-1}{2} d\left(\frac{u}{a}\right)_3 = d\lambda_3^- \\ Q'_L = Q'_R \\ h'_{0L} = h'_{0R} \\ p_{0R} - p_{0L} = \rho_L (u_L - V_{tr})^2 \xi_{nt}/2 \\ Q_1 = Q_L + Q_3 \\ p_{01} - p_{0L} = \rho_L u_L^2 \xi_{12}/2 \\ p_{01} - p_{03} = \rho_3 u_3^2 \xi_{13}/2 \\ h_{01} = h_{0L} = h_{03} \end{cases} \tag{14,15}$$

where ξ_{nt} denotes the stagnation pressure loss coefficient of the train-nose, and the prime, a frame of reference relative to train. The unknowns that have to be solved are u, c and a at sections L, R, 2 and 3 for case (a), and at sections 1, L, R and 3 for case (b).

For the train rear-junction interaction, the same principle can be used. The zone L-R is treated in the same way. Meanwhile, the suction effect of the rear of the train generates a joining flow at the junction. Consequently in the zone 1-2-3, the stagnation enthalpy balance must be used instead of expressing the equality of the specific stagnation enthalpy at sections 1, 2, and 3.

The body-junction interaction can be modelled in the same manner as the wave-junction interaction, by noting that tunnel's cross section is replaced by the annulus cross section when expressing the conservation of mass and the stagnation enthalpy balance.

The systems obtained for all these boundaries are difficult to solve directly. It has been stated (William-Louis, 1994) that they are unstable in the sense that several numerical solutions can be obtained and among them non-physical ones. Actually, these solutions depend strongly on the initialisation of the iteration process. The use of the "branch superposition method" for solving these systems leads to an unique and physical solution (William-Louis and Tournier, 1996) which will only depend on the flow conditions in the boundary.

For a brief description of this method, consider the system of equations (5) to (13). This system is uncoupled into two systems noted S_1 and S_2. S_1 is formed by equations (5), (6), (9), (10), (11) and (12), while S_2 is formed by (7), (8) and (13). The solution procedure consists of solving S_1 and S_2 by an interation process in two steps.

- First, the system S_1 is solved by keeping constant the conditions at section 3 to give a primary solution for the conditions at sections 1 and 2.
- In the second step, the previous solution of the system S_1 is used as data for the system S_2 which is solved to obtain new values of the conditions at section 3. These new values are used as data for solving again the system S_1 as described in the first step.

Contact surface

When the rear enters in the tunnel, a suction effect is produced which makes the air flow from atmosphere into the tunnel. This incoming air is separated by a contact surface from the air in the tunnel which has already received mechanical energy from the train. This discontinuity moves with the local fluid velocity and needs to be treated as a boundary within the method of characteristics solution. The application of this method on both sides of the contact surface (noted sections L and R) leads to four compatibility relations along C_L^+, C_L^0, R_R^-, and C_R^0.

The velocity and the pressure are continuous across this surface resulting in the following governing equations

$$\begin{cases} d\left(\frac{c}{a}\right)_L + \frac{\gamma-1}{2} d\left(\frac{u}{a}\right)_L = d\lambda_L^+ \\ \frac{1}{a_L}\left(\frac{da}{dt}\right)_L = \frac{\gamma-1}{2c_L^2}\left(P+\dot{Q}\right)_L \\ d\left(\frac{c}{a}\right)_R - \frac{\gamma-1}{2} d\left(\frac{u}{a}\right)_R = d\lambda_R^- \\ \frac{1}{a_R}\left(\frac{da}{dt}\right)_R = \frac{\gamma-1}{2c_R^2}\left(P+\dot{Q}\right)_R \\ u_L = u_R \\ c_L/a_L = c_R/a_R \end{cases} \tag{16}$$

where the unknowns that have to be solved are u, c and a at sections L and R.

Contact surface-junction interaction

The contact surface-junction boundary can be handled in the same manner as shown in Figure 2 (case a). Noting that the suction effect of the rear of the train generates a joining flow in the junction, only four sections are involved for the

calculation: sections L, R, 2 and 3. As a result, six characteristics can be constructed: C_L^+, C_L^0, C_R^0, C_3^0, C_3^+ and C_2^-.

In the zone R-2-3, the equations (10) to (13) can be used. The constancy of pressure and velocity across the contact surface gives two relations. Finally, these equations are solved in conjunction with the compatibility conditions by the "branch superposition method".

To the knowledge of the authors, no practical information appears to be available on the behaviour of the contact surface as it passes through the junction. When the contact surface reaches the junction, however, it is assumed that it is merged into the general flow by vigorous mixing owing to turbulence. As result, the calculation proceeds without the contact surface downstream to the junction.

Results and discussion

Validation

In this section, two kind of tunnels are considered: a simple one (Patchway tunnel, see Table I) and a second with an airshaft located at 283.9m from the tunnel entry portal (Table II). Full scale experimental measurements have been carried out in these tunnels (Gawthorpe and Pope, 1993; Woods and Pope, 1981) and have been used by other authors to validate their prediction methods. They are also employed here to validate the prediction method presented in this paper.

Figure 3 shows the pressure fluctuations with time at 500m from the tunnel entry portal compared with calculation for a train running at 34.7m/s. Good agreement is obtained. Phase discrepancies are noted with increasing time after the waves pass through the annulus. This behaviour is identical to that

	Tunnel		Train	
x (m)	A (m^2)	Perimeter (m)	A (m^2)	Perimeter (m)
0	22.61	18.19	8.2	9.82
100	21.84	17.68	8.2	9.82
300	23.09	18.06	–	–
500	22.32	17.95	–	–
900	23.32	18.38	–	–
1,140	25.65	19.19	–	–

Table I.
Patchway tunnel test

	Tunnel		Train		Airshaft	
x (m)	A (m^2)	Perimeter (m)	A (m^2)	Perimeter (m)	A (m^2)	Perimeter (m)
0	38	23.87	8.2	9.82	5.94	8.64
30	38	23.87	8.2	9.82	5.94	8.64
100	38	23.87	8.2	9.82	–	–
1,218	38	23.87	–	–	–	–

Table II.
Tunnel with airshaft test

displayed by prediction methods developed by other authors and is due probably to two effects:

(1) the friction and the heat exchanges being important in the annulus and modifying the local speed of sound;

(2) the assumption that zones where three dimensional effects are predominant are infinitesimally thin.

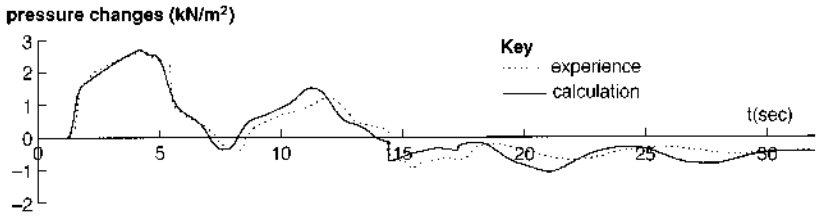

Figure 3.
Patchway tunnel. Pressure excursion at 500m from entry portal

The latter gives rise to a quasi-instantaneous transmission or reflection of the waves on both sides of the zones which can introduce a temporal shift. Indeed an analysis performed by Schultz and Sockel (1991) for short tunnels in which allowance is made for three dimensional pressure field effects at the ends of the train and tunnel shows much improved levels of agreement between theory and experiment.

In Figure 3, one can identify three sequential effects associated with the entry of the train:

- an initial first rise in pressure due to the passage of the initial train-nose entry wave front;
- a gradual rise in pressure due to wall friction as the train draws into the tunnel;
- a fall in pressure, resulting from the generation of an expansion wave as the rear of the train enters the tunnel.

These waves propagate along the tunnel at the speed of sound. When they reach the ends of the tunnel they are reflected as waves of opposite sign. As the waves propagate back and forth along the tunnel, they are progressively attenuated by wall friction and the dissipation of energy which occurs each time the waves are reflected at the ends of the tunnels.

The results for a train running at 38.9m/s in a tunnel with an airshaft are illustrated in Figure 4. Tests were conducted with the airshaft blocked (case (a)) and open (case (b)). Blocking the shaft creates a simple tunnel. In both cases, good agreement is noted between numerical results and measured pressure excursions at 251m from the tunnel entry portal. An interesting feature of case (b) is the influence of the shaft on the pressure waves. In case (b) the maximum pressure variation is reduced by 30 per cent. When the initial wave front reaches the junction, it divides into three secondary waves. One of them is

reflected as an expansion wave and propagated back to the tunnel entry. This wave arrests the linear increase in pressure by accelerating the air flow in front of the train.

Figure 5 illustrates the complete propagation process. The cases (a) and (b) show the spatial and temporal variations in pressure respectively for the two configurations of tunnel described previously (with blocked shaft and with open shaft). The cases (c) and (d) present the equivalent temperature field for both configurations of tunnel.

The wave trajectories and the pressure and temperature fluctuations can be readily differentiated. On (c) and (d), the contact surface is clearly shown as a temperature discontinuity, which allows transmission of the pressure waves through it. Between this contact surface and the tunnel entry, the temperature does not differ much to the atmospheric value. The temperature changes, however, are much more pronounced between this surface and the train rear. In this part, air is qualified to be "hot" because it has already received mechanical energy from the train, and over this, the waves cause changes in the temperature. At the front of the train, the temperature fluctuations result only from the passage of waves which locally modify the thermal behaviour of the flow. This is why a similarity is noted between the temperature and pressure fields in this part of the tunnel.

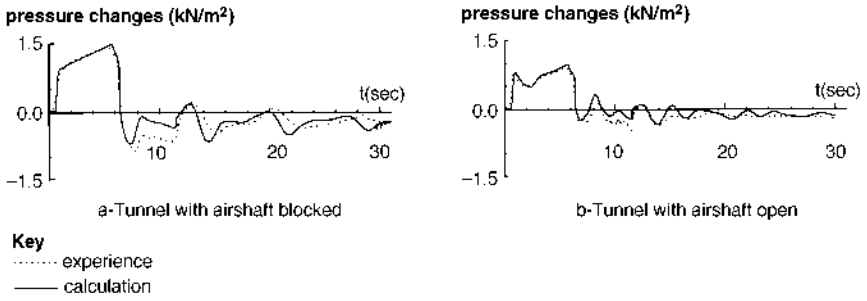

Figure 4.
Pressure excursion at 251m from entry portal (airshaft position: 283.9m)

Numerical simulations illustrating the effects of airshafts

In this part, the influence of airshafts on the pressure waves is discussed. Pressure excursions at 251m from the tunnel entry are plotted in Figures 6, 7, 8a, 9 and 10.

Figure 6 shows that the shaft's location can modify the maximum pressure change at the measuring point. Moving the shaft away from tunnel entry increases the propagation time of the reflected expansion. In general, it appears to be preferable to bring the shaft nearer to the tunnel entry when reducing the maximum pressure changes. The position must be far enough from the entrance to permit the initial wave to develop fully otherwise there is some loss of benefit.

In Figure 7, it is noted that the expansion, after the passage of the initial wave front, is all the more important if the shaft is short (the models presented in this

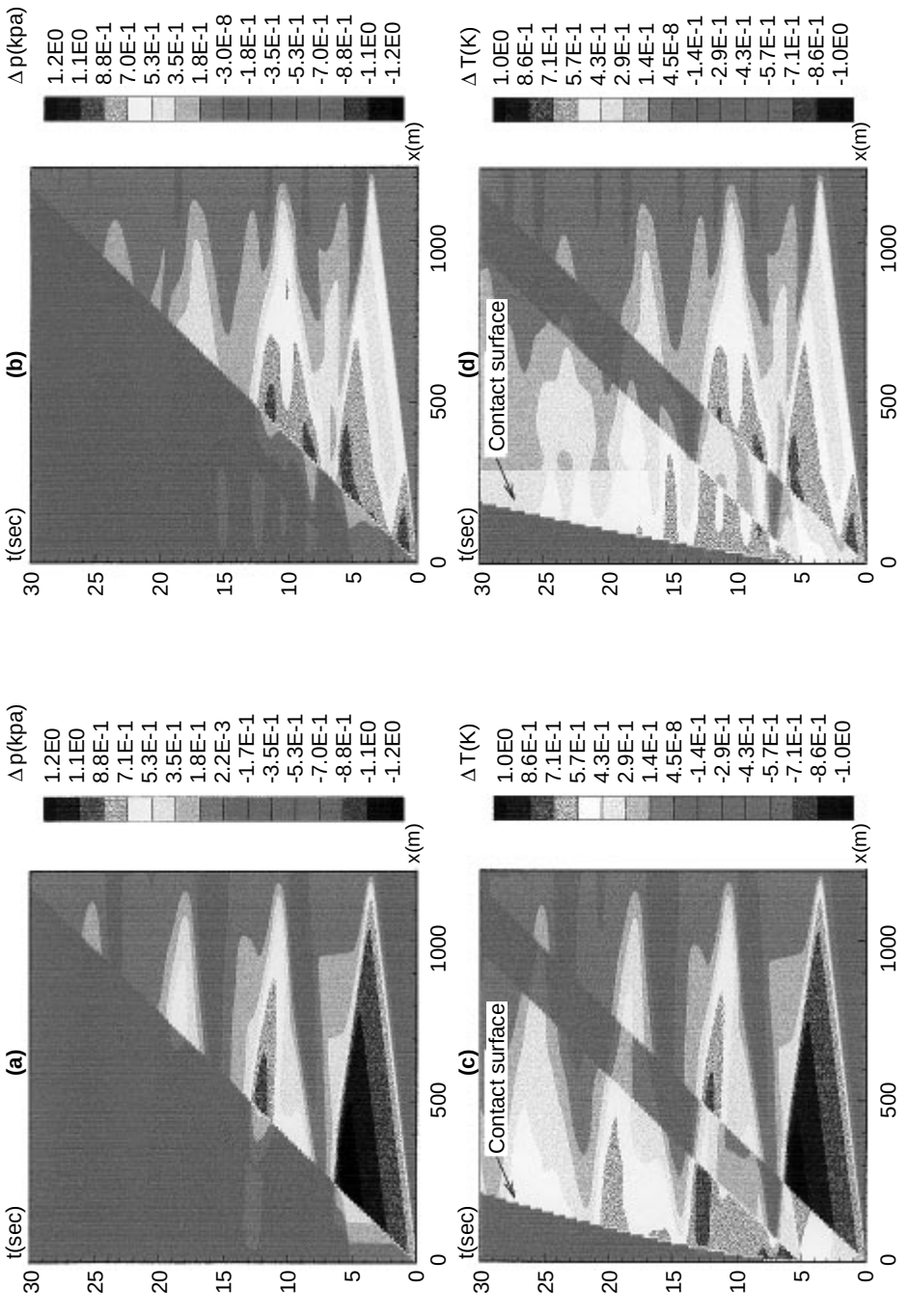

Figure 5.
Pressure (a, b) and temperature fields (c, d) in tunnel with blocked shaft (a, c) or open shaft (b, d)

study are valid only for shafts of zero length). The train-nose wave front divides into three parts when it interacts with the junction. An expansion, A, is reflected back to the tunnel entry and a compression wave is transmitted both along the tunnel and through the shaft. The last part is reflected at the shaft exit and returns to the junction as an expansion wave which divides also into three parts. One part (expansion noted B) is transmitted and propagated towards the tunnel entry. The delay between A and B , therefore, depends on the shaft's length. Consequently, the smaller this delay, the stronger the expansion resulting from the superposition of A and B and the greater the fall in pressure after the passage of the initial wave front.

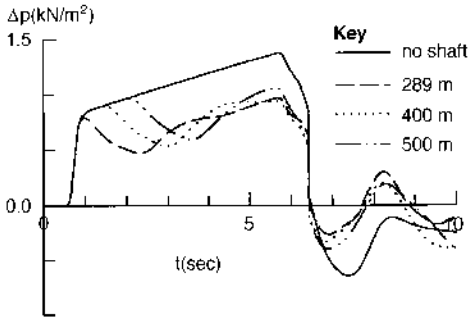

Figure 6.
Influence of the shaft's position

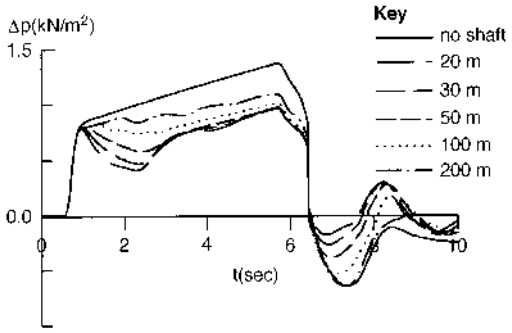

Figure 7.
Influence of the shaft's length

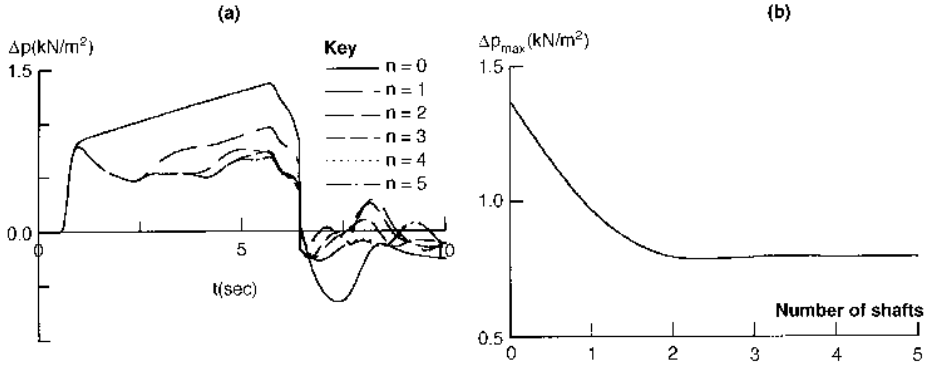

Figure 8.
Influence of the number of shafts

In increasing the number of shafts, it can be seen that the maximum pressure change falls to approximately the strength of the nose-entry wave (Figure 8). The presence of a junction results in the division of a wave into secondary waves of weaker intensity. Adding junctions increases the multiplicity of these secondary waves. There comes a point, however, when adding further shafts ceases to provide additional reductions in the peak wave strength. In the present study, this threshold is reached when there are three shafts (Figure 8b).

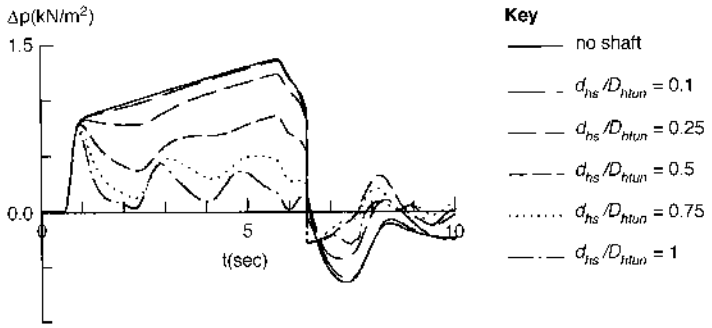

Figure 9.
Influence of the ratio d_{hs}/D_{htun}

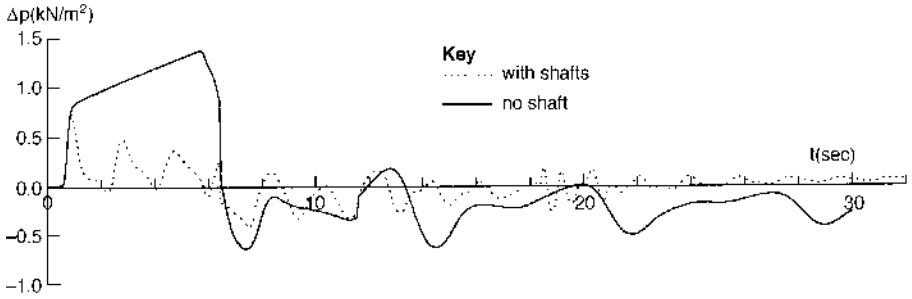

Figure 10.
Example of pressure wave damping by airshafts

There is a reduction in the maximum pressure change as the ratio of the shaft and tunnel hydraulic diameters represented here by $\frac{d_{hs}}{D_{htun}}$ (where d_{hs} and D_{htun} are respectively the shaft and the tunnel hydraulic diameters) increases (Figure 9).

For small ratios, the energy loss when the fluid flows into the shaft is large and consequently the wave which is transmitted into the branch is weak. In this case, the part which is transmitted along the tunnel ahead of the junction is the more significant component. For very small ratios, the wave is almost completely transmitted downstream of the junction and the airshaft behaves like a tunnel perforation. Conversely, when this ratio increases, the division of the wave results in the expansion wave which is reflected back to the tunnel entry becoming much stronger and having a much more significant effect on attenuating the pressure changes generated by the train running into the tunnel.

To illustrate the benefit in using shafts, three identical shafts are considered. They are 20m long and spaced at 200m intervals. The cross-sectional ratio $\frac{d_{hs}}{D_{htun}}$ is taken to be equal to unity. For these conditions, Figure 10 shows that the waves are highly attenuated with the maximum pressure changes reduced by 45 per cent.

Conclusion

The non-homentropic flow model has been extended to the case of trains running in tunnels with airshafts. Comparison of numerical results with experimental measurements shows good agreement for a simple tunnel and for a tunnel with an airshaft. The results confirm that the use of shafts provides a very effective method for reducing pressure fluctuations in tunnels. The shafts divide the waves into secondary waves which can be more effectively damped by viscous dissipation or acoustic diffusion.

In further work, it would be useful to study the behaviour of contact surface in a junction and its interaction with a train. This would be an important step in the extension of the non-homentropic models to multiply connected tunnel configurations with passing trains.

References

Fox, J.A. and Henson, D.A. (1971), "The prediction of the magnitude of pressure transients generated by a train entering a single tunnel", *Proc. Inst. Civ. Engrs*, Vol. 49, May, pp. 53-69.

Fox, J.A. and Vardy, A.E. (1973), "The generation and alleviation of air pressure transients caused by the high speed passage of vehicles through tunnels", *ISAVVT*, organised by the BHRA Fluid Engineering, Cranfield, held in Canterbury, 10-12 April.

Gawthorpe, R.G. and Pope, C.W. (1993), "Reduced cross sections for high speed tunnels in shallow ground using airshafts", *STECH*, Vol. II, 22-26 November, Yokohama, Japan, pp. 195-8.

Hammitt, A.G. (1975), "Unsteady aerodynamics of vehicles in tubes", *AIAA Journal*, Vol. 13 No. 4, April, pp. 497-503.

Henson, D.A. *et al.* (1982), "Aerodynamics and ventilation of a proposed channel tunnel", *4th ISAVVT*, organised by the BHRA Fluid Engineering, Cranfield, held in York, 23-25 March.

Pichard, J. (1989), "Ecoulements variés", *Techniques de l'Ingénieur*, Vol. A.732, pp. 1-12.

Pope, C.W. (1986), "Gas dynamics and thermodynamics of unsteady flow in a railway tunnel", thesis, The Open University, Milton Keynes, April.

Schultz, M. and Sockel, H. (1988), "The influence of unsteady friction on the propagation of pressures waves in tunnels", *6th ISAVVT*, organised by the BHRA Fluid Engineering, Cranfield, 27-29 September, Durham, pp. 123-35.

Schultz, M. and Sockel, H. (1991), "Pressure transients in short tunnels", *7th ISAVVT*, organised by the BHRA Fluid Engineering, Cranfield, held in Brighton, 27-29 November, paper C1.

Vardy, A.E. (1976), "The use of airshafts for the alleviation of pressure transients in tunnels", *2nd ISAVVT*, organised by the BHRA Fluid Engineering, Cranfield, held in Cambridge, 23-25 March, paper C4.

Waclawicek, M.E. and Sockel, H. (1982), "Pressure transients and aerodynamic power in railway tunnels with special reference to airshafts and entropy", *4th ISAVVT*, organised by the BHRA Fluid Engineering, Cranfield, held in York, 23-25 March, paper H1.

William-Louis, M. (1994), "Etude aérothermodynamique de la propagation des ondes de pression lors de la circulation des trains en tunnels simples ou ramifiés", Thèse, Université de Valenciennes, France.

William-Louis, M. and Tournier, C. (1996), "Calculation of pressure wave propagation through a tube junction", *Journal of Mechanical Engineering Science (IMech)*, part C, Vol. 210, pp. 239-44.

William-Louis, M., Tournier, C. and Crnojevic, C. (1993), "Theoretical evaluation of the friction coefficient in the zone between a train and a tunnel: application to the propagation of pressure waves", *ITTG*, Vol. II, Lille-France, pp. 1025-35.

Woods, W.A. and Pope, C.W. (1979), "On the range of validity of simplified one dimensional theories for calculating unsteady flows in railway tunnels", *3rd ISAVVT*, organised by the BHRA Fluid Engineering, Cranfield, held in Sheffield, 19-21 March, paper D2.

Woods, W.A. and Pope, C.W. (1981), "A generalised flow prediction method for the unsteady flow generated by a train in a single-track tunnel", *Journal of Wind Engineering and Industrial Aerodynamics*, Vol. 7, pp. 331-60.